Impact of inclined outer velocity in MHD Casson fluid over stretching sheet

Renu Devi[1], Vikas Poply[*,2], Manimala[3]
renu15dahiya@gmail.com vikaspoply@gmail.com manimala@ansaluniversity.edu.in
[1,3]Department of Mathematics, Ansal University, Gurgaon-122017, India
[2]Department of Mathematics, KLP College, Rewari-123401, India
Corresponding Author's email id: vikaspoply@gmail.com

Abstract

This manuscript discuss the influence of inclined outer velocity on heat and flow transference in boundary layer Casson fluid over stretching sheet. The flow is adopted to have magnetic field in the uniform manner on stretching surface. It has been taken that in both directions along the horizontal axis, the sheet is stretched. Using similarity transformations, the generating equations representing the heat and flow transportation are converted to ordinary differential equations. The flow is influenced by magnetic parameter, Casson fluid parameter, Prandtl number and the impinging angle parameter. The numerical solutions of the transformed equations have been computed by the Runge-Kutta Fehlberg method using shooting procedure. Behavior of emerging parameters is depicted graphically. Acceptance of the extant technique used in current study is correlated with the existing outcomes.

Keywords: Casson fluid; MHD; outer velocity; oblique flow.

1 Introduction

Numerous practical applications of heat and flow transportation in several divisions of manufacturing procedure lead attention of many researchers in this field of stretching surface. Crane [1] initiated the work on stretching surface by analyzing the heat and flow characteristics over stretching sheet. Many researchers [2–4] further extended this study by analyzing the impact on flow characteristics in various situations and different surfaces, where theoretical results are covenant with experimental results and they are well documented in the literature. But, in some real-world application such as extrusion of sheet, fluid has some prescribed velocity. Many researcher analyzed the effect of the outer velocity and stagnation-point flow over stretching surfaces [5–13].

Many biological as well as industrial driven fluid such as multi-tude oils, lubricating greases, gypsum pastes, cleansing agents, blood, ceramics, paints etc., flow behavior does not pertained to the theory of Newtonian fluid and its extensions. Therefore, numerous work have been done for non-Newtonian fluids, such as viscoelastic fluid [14, 15] and power-law fluid [16].

The Casson fluid model containing several food stuffs and biological materials, especially blood. Mustafa et al. [17] analyzed the behavior of heat and flow transportation of Casson fluid about a stagnation point using Homotopy analysis method (HAM). Duality and exactness of the solution in Casson fluid has been observed in [18] and [19] respectively. They stated that the dual solution exist in shrinking sheet as well as in stretching sheet. In Casson fluid, Sheikh and Abbas [20] discussed the influence of homogenous and heterogeneous reactions emerged from uniform suction and slip from the surface. Effect of slip velocity on unsteady stretching sheet due to Casson fluid with variable heat flux has been examined by Megahed [21].

The above literature survey reveals that no study had discussed so far the impact of magnetic field on oblique stagnation point with outer velocity over a stretching surface in Casson fluid flow. The purpose of current analysis over stretching sheet is to examine the combined influence of inclined outer velocity and Casson fluid over heat and flow transportation in MHD flows.

2 Mathematical Formulation

Steady 2D Casson fluid flow of a non-compressible, viscous, electrical conducting fluid with outer flow is considered. $u_w(x)$ and T_w are the linear velocity and uniform temperature on stretching surface respectively. The generating equations of flow under the above assumptions are described as:

$$\frac{\partial u}{\partial x}+\frac{\partial v}{\partial y}=0 \tag{1}$$

$$u\frac{\partial u}{\partial x}+v\frac{\partial u}{\partial y}=-\frac{1}{\rho}\frac{\partial P}{\partial x}+\nu\left(1+\frac{1}{\beta}\right)\left(\frac{\partial^2 u}{\partial x^2}+\frac{\partial^2 u}{\partial y^2}\right)-\frac{\sigma B_0^2 u}{\rho} \tag{2}$$

$$u\frac{\partial v}{\partial x}+v\frac{\partial v}{\partial y}=-\frac{1}{\rho}\frac{\partial P}{\partial y}+\nu\left(1+\frac{1}{\beta}\right)\left(\frac{\partial^2 v}{\partial x^2}+\frac{\partial^2 v}{\partial y^2}\right) \tag{3}$$

$$\left(u\frac{\partial T}{\partial x}+v\frac{\partial T}{\partial y}\right)=\frac{K}{\rho C_P}\frac{\partial^2 T}{\partial y^2} \tag{4}$$

where velocity along y (vertical axis) and x (horizontal axis) - axes are taken as v and u respectively. P,ν,σ,C_P,T,Q,K and B_0 denotes the pressure, kinematic viscosity, electrical conductivity, specific heat (at constant pressure), fluid temperature, thermal conductivity and magnetic field strength of the fluid respectively.

Restrictions on the boundary are describing the flow model as:

$$\left(\begin{array}{l}\text{At } \ y=0,\ \ u=u_w\left(x\right)=bx,\ \ v=0,\ T=T_w\\ \text{As } \ y\to\infty,\ \ u=nx\ sin\gamma+mycos\gamma,\ \ v=-nysin\gamma,\ \ T=T_\infty\end{array}\right) \tag{5}$$

where b, n and m are non-negative invariable values of dimension (time^{-1}). The fluid having unvarying temperature T_∞ very far from the surface and γ is impinging angle from the x -axis, at which Casson fluid striking the stretching sheet (striking angle parameter). After removing (P) from equations (2) and (3), we obtained

$$\frac{\partial u}{\partial y}\frac{\partial u}{\partial x}+u\frac{\partial^2 u}{\partial x\partial y}+\frac{\partial v}{\partial y}\frac{\partial u}{\partial y}+v\frac{\partial^2 u}{\partial y^2}-\frac{\partial u}{\partial x}\frac{\partial v}{\partial x}-u\frac{\partial^2 v}{\partial x^2}-\frac{\partial v}{\partial x}\frac{\partial v}{\partial y}=\nu\left(1+\frac{1}{\beta}\right)v\frac{\partial^2 v}{\partial x\partial y}\left(\frac{\partial^3 u}{\partial y\partial x^2}+\frac{\partial^3 u}{\partial y^3}-\frac{\partial^3 v}{\partial x^3}-\frac{\partial^3 v}{\partial x\partial y^2}\right)-\frac{\sigma B^2}{\rho}\frac{\partial u}{\partial y} \tag{6}$$

Introducing $\xi=\sqrt{\frac{b}{\nu}}x,\ \eta=\sqrt{\frac{b}{\nu}}y$ and $\psi\left(\xi,\eta\right)$ (stream function) as dimensionless variables such that $u=\frac{\partial\psi}{\partial\eta}$ and $v=-\frac{\partial\psi}{\partial\xi}$. The Boundary condition in term of stream function $\psi\left(\xi,\eta\right)$ is given by,

$$\left(\begin{array}{l}\psi=0,\quad \frac{\partial\psi}{\partial\eta}=\xi\quad \text{on}\quad \eta=0\\ \psi=\lambda\xi\eta sin\gamma+\frac{1}{2}R\eta^2cos\gamma\quad \text{as}\quad \eta\to\infty\end{array}\right) \tag{7}$$

where $\lambda=\frac{n}{b}$ is outer velocity parameter and $R=\frac{m}{b}$ is some positive constant.

We need solution of equation (6) from the relation $\psi=\xi f_0\left(\eta\right)+g_0\left(\eta\right)$, where $g_0\left(\eta\right)$ and $f_0(\eta)$ are referred as tangential and normal part of the flow. Also, $v=-f_0\left(\eta\right)$ and $u=\xi f_0^{'}\left(\eta\right)+g_0^{'}\left(\eta\right)$.

Equation (1) is contented by given v and u and equation (6) transformed to,

$$f_0^{'}(\eta)\left[\xi f_0^{''}(\eta)+g_0^{''}(\eta)\right]+\left[\xi f_0^{'}(\eta)+g_0^{'}(\eta)\right]f_0^{''}(\eta)-f_0^{'}(\eta)\left[\xi f_0^{''}(\eta)+g_0^{''}(\eta)\right]-f_0(\eta)\left[\xi f_0^{'''}(\eta)+g_0^{'''}(\eta)\right]= \left(1+\tfrac{1}{\beta}\right)\left[\xi f_0^{''''}(\eta)+g_0^{''''}(\eta)\right]-M\left[\xi f_0^{''}(\eta)+g_0^{''}(\eta)\right] \tag{8}$$

Here $M=\frac{\sigma B_0^2}{b\rho}$ is the Chandershekhar number (magnetic parameter). Also, comparing the coefficient of ξ and ξ^0, we get

$$\left(1+\frac{1}{\beta}\right)f_0^{''''}(\eta)+f_0(\eta)f_0^{'''}(\eta)+f_0^{'}(\eta)f_0^{''}(\eta)-2f_0^{'}(\eta)f_0^{''}(\eta)-Mf_0^{''}(\eta)=0 \tag{9}$$

$$\left(1+\frac{1}{\beta}\right)g_0^{''''}(\eta)+f_0^{'}(\eta)g_0^{''}(\eta)+f_0(\eta)g_0^{'''}(\eta)-f_0^{'}(\eta)g_0^{''}(\eta)-g_0^{'}(\eta)f_0^{''}(\eta)-Mg_0^{''}(\eta)=0 \tag{10}$$

After integrating, equation (9) and (10) become

$$\left(1+\frac{1}{\beta}\right)f_0^{'''}(\eta)+f_0(\eta)f_0^{''}(\eta)-\left(f_0^{'}(\eta)\right)^2-Mf_0^{'}(\eta)+C=0 \tag{11}$$

$$\left(1+\frac{1}{\beta}\right)g_0^{'''}(\eta)+f_0(\eta)g_0^{''}(\eta)-f_0^{'}(\eta)g_0^{'}(\eta)-Mg_0^{'}(\eta)+D=0 \tag{12}$$

where C and D are constant of integration and determined by boundary condition,

$$\begin{aligned} &f_0(0)=0, \quad f_0^{'}(0)=1, \quad f_0^{'}(\infty)=\lambda sin\gamma \\ &g_0(0)=0, \quad g_0^{'}(0)=0, \quad g_0^{''}(\infty)=\ R\ cos\gamma \end{aligned} \tag{13}$$

Incorporating value of C and D in equations (11) and (12) respectively, we get

$$\left(1+\frac{1}{\beta}\right)f_0^{'''}(\eta)+f_0(\eta)f_0^{''}(\eta)-\left(f_0^{'}(\eta)\right)^2-M\left[f_0^{'}(\eta)-\lambda sin\gamma\right]+(\lambda sin\gamma)^2=0 \tag{14}$$

$$\left(1+\frac{1}{\beta}\right)g_0^{'''}(\eta)+f_0(\eta)g_0^{''}(\eta)-f_0^{'}(\eta)g_0^{'}(\eta)-M\left(g_0^{'}(\eta)-R\eta cos\gamma\right)-\alpha Rcos\gamma=0 \tag{15}$$

Further, we find that the linearity of equation (15) can take the solution of the form

$$g_0^{'}(\eta)=kcos\gamma h_0(\eta) \tag{16}$$

where, $h_0(\eta)$ is define from the equation

$$\left(1+\frac{1}{\beta}\right)h_0^{''}(\eta)+f_0(\eta)h_0^{'}(\eta)-f_0^{'}(\eta)h_0(\eta)-M\left(h_0(\eta)-\eta\right)-\alpha=0 \tag{17}$$

$$h_0(0)=0, \quad h_0^{'}(\infty)=1 \tag{18}$$

By considering the normal component of the flow field, the dimensionless temperature $\theta\left(\eta\right) = \frac{(T-T_\infty)}{(T_w-T_\infty)}$. Substituting $\theta\left(\eta\right)$ in equation (4), we get

$$\theta^{''}(\eta) + Pr\theta^{'}(\eta)f_0(\eta) + Pr\theta(\eta) = 0 \tag{19}$$

where $Pr\left(=\frac{\mu C_P}{K}\right)$ is Prandtl number. Corresponding boundary conditions of (5) reduces to,

$$\theta\left(0\right) = 1, \quad \theta\left(\infty\right) = 0 \tag{20}$$

3 Results and Discussion

Runge-Kutta Fehlberg has been used to solve numerically the equations (14), (17) and (19) with their corresponding boundary conditions through shooting technique. Table 1 demonstrates the numerical algorithm applied for the current problem is in favorable justification with published work and thus validating the model and numerical algorithm. Velocity and dimensionless temperature of the model have been acquired for distinct entries of outer velocity parameter λ, Casson fluid parameter β, striking angle parameter γ, magnetic parameter (Chandershekhar number) M. In order to get insights of the fluid behavior, the graphs have been inserted to evaluate the influence of numerous fluid parameters on heat and flow transportation. The value of horizontal axis $-\eta$ is chosen so that velocity profiles and temperature profiles asymptotic tends to the boundary condition. All the simulations are carried with $\eta_{max} = 10$. However, to depict the characterization of curve effectively, much lower values of η are used.

The impact of β on profiles of velocity for outer velocity parameter $\lambda = 0.5$ and $\lambda = 1.5$ as displayed

Table 1: $f_0''(0)$ for distinct entries of λ at large β, a comparison.

λ	Present paper	Singh et.al [6]	Lok et.al. [22]
0	-0.969386	-0.976371	-0.969388
0.1	-0.918107	-0.921594	-0.918110
0.5	-0.667263	-0.667686	-0.667271
2	2.017502	2.0174763	2.017615

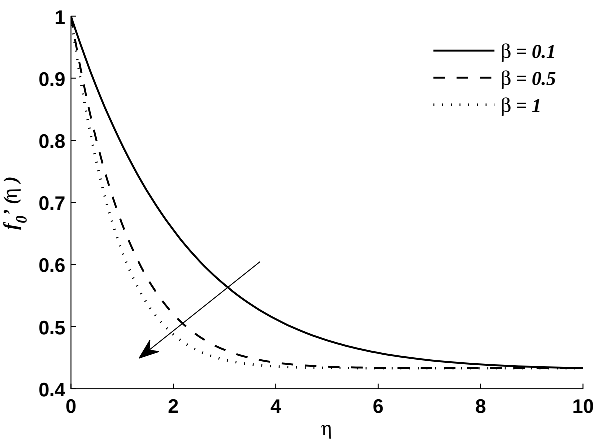

Figure 1: $f_0'(\eta)$ for distinct β, when $M = 0.5$, $R = 1$, $Pr = 0.71$, $\gamma = \pi/3$ and $\lambda = 0.5$.

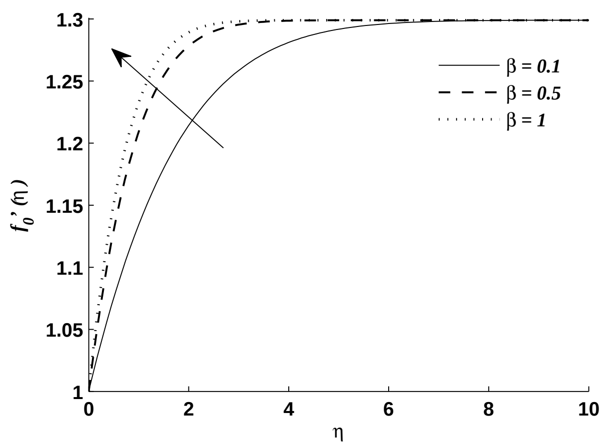

Figure 2: $f_0'(\eta)$ for distinct β, when $M = 0.5$, $R = 1$, $Pr = 0.71$, $\gamma = \pi/3$ and $\lambda = 1.5$.

by the Figures 1 and 2 respectively. Physically, $\lambda < 1$ explained by the case when stretching sheet velocity exceeds the outer velocity. Figure 1 shows that a reduction in fluid velocity has been observed with the rise in β for $\lambda = 0.5$. This behavior is explained by the fact that, increasing the non-Newtonian Casson fluid parameter β yields increment in the fluid stress causing a resistance force which declines the fluid velocity. For large value of β, decrease in boundary layer thickness is noticed for $\lambda = 0.5$ (Figure 1). In Figure 2, velocity profile curves increases along with the increase in β for $\lambda > 1$. An inverted boundary layer is formed in velocity profile in Figure 2 for $\lambda > 1$. An opposite trends of velocity profile has been observed for $\lambda = 1.5$ in Figure 2 in comparison with $\lambda = 0.5$ (shown by Figure 1).

Figures 3 - 4 show the profiles of temperature curves when Casson fluid parameter $\beta = 0.1, 0.5$ and

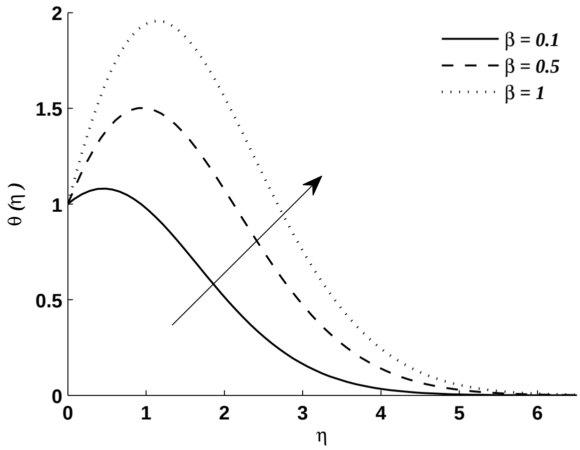

Figure 3: $\theta(\eta)$ for distinct β, when $M = 0.5$, $R = 1$, $Pr = 0.71$, $\gamma = \pi/3$ and $\lambda = 0.5$.

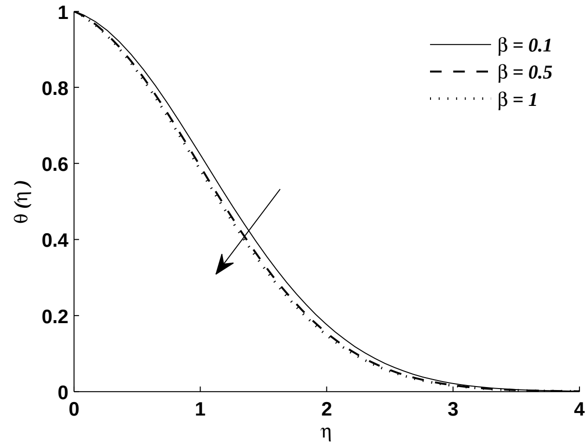

Figure 4: $\theta(\eta)$ for distinct β, when $M = 0.5$, $R = 1$, $Pr = 0.71$, $\gamma = \pi/3$ and $\lambda = 1.5$.

1 in presence of $\lambda < 1$ and $\lambda > 1$ respectively. For a fixed β in Figure 3, firstly the temperature curve increases and it shows a decline in curve after some distance η. This change in the behavior of temperature curve is due to the presence of β. Also, Figure 3 reveals that increase in temperature has been observed with the increase in β for $\lambda < 1$. As explained in above paragraph that as Casson fluid parameter increases, fluid velocity decrease which results in low heat transfer rate and hence temperature increase for $\lambda = 0.5$. Opposite trend in velocity profiles for $\lambda < 1$ is the reason for decrease in temperature profiles in the case for $\lambda > 1$ (shown in Figure 4). However, the thermal boundary thickness is thinner for $\lambda > 1$ as compared to that of $\lambda < 1$. Graphs of Velocity for distinct entries of M for $\lambda = 0.5$ and $\lambda = 1.5$ are depicted by

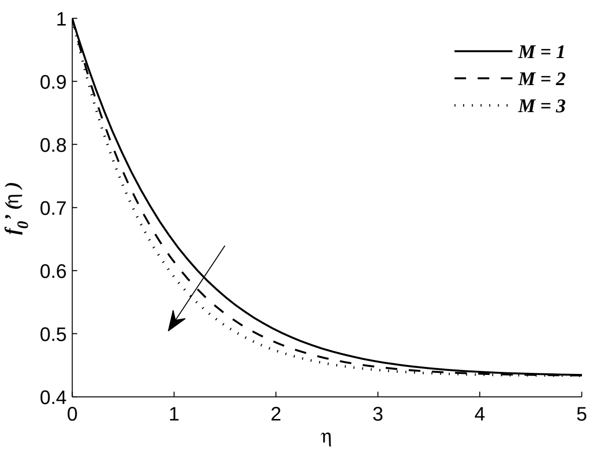

Figure 5: $f_0'(\eta)$ for distinct M, when $\beta = 0.5$, $R = 1$, $Pr = 0.71$, $\gamma = \pi/3$ and $\lambda = 0.5$.

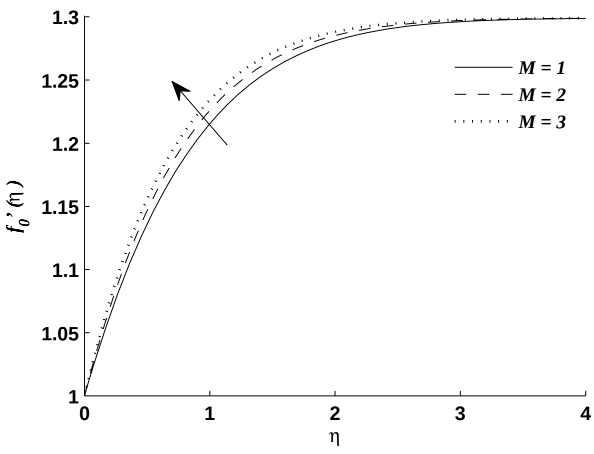

Figure 6: $f_0'(\eta)$ for distinct M, when $\beta = 0.5$, $R = 1$, $Pr = 0.71$, $\gamma = \pi/3$ and $\lambda = 1.5$.

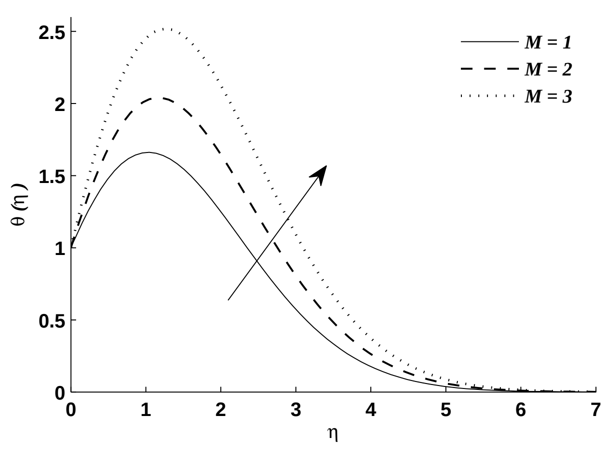

Figure 7: $\theta(\eta)$ for distinct M, when $\beta = 0.5$, $R = 1$, $Pr = 0.71$, $\gamma = \pi/3$ and $\lambda = 0.5$.

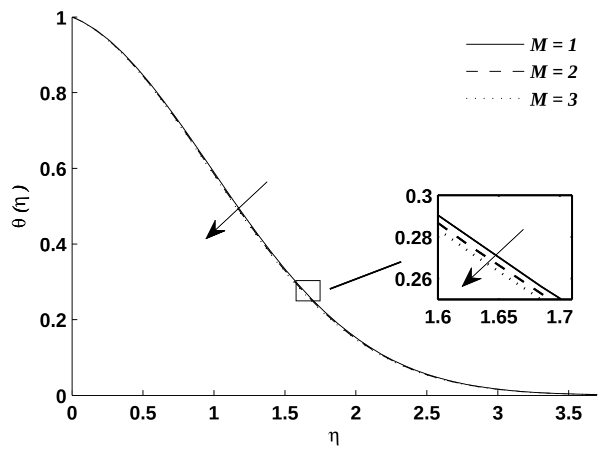

Figure 8: $\theta(\eta)$ for distinct M, when $\beta = 0.5$, $R = 1$, $Pr = 0.71$, $\gamma = \pi/3$ and $\lambda = 1.5$.

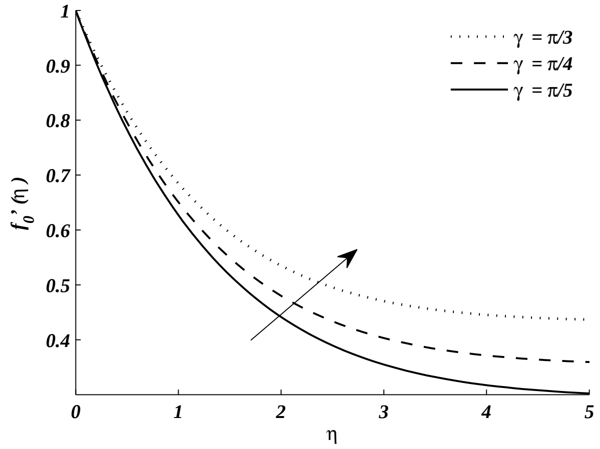

Figure 9: $f_0'(\eta)$ for distinct γ, when $M = 0.1$, $\beta = 0.5$, $R = 1$, $Pr = 0.71$ and $\lambda = 0.5$.

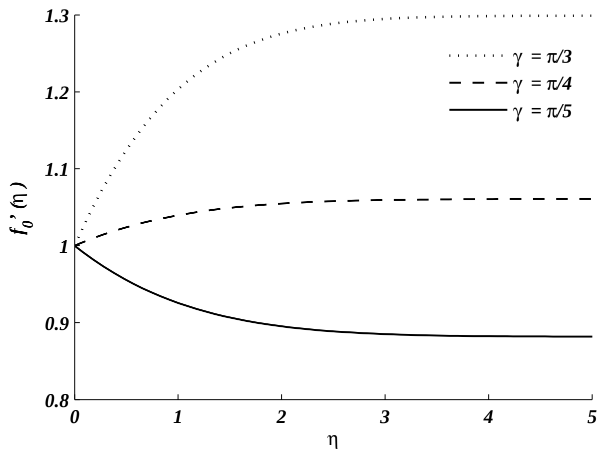

Figure 10: $f_0'(\eta)$ for distinct γ, when $M = 0.1$, $\beta = 0.5$, $R = 1$, $Pr = 0.71$ and $\lambda = 1.5$.

the Figures 5 and 6 respectively. Figure 5 shows that a reduction in velocity is noticed with increasing M. Physically this behavior has been explained as, the magnetic field can induce current on conducting fluid and the transverse magnetic field behaves like a Lorentz force, which produce retardation on fluid boundary layer and the fluid velocity slow down due to the retardation. Consequently, momentum thickness reduces. Hence, fluid magnetism is used to control the desired formation of final object. Figure 6 demonstrates that as M increases, velocity increases for $\lambda = 1.5$.

Figures 7 and 8 display the profiles of temperature with variation in the entries of Chandershekhar number M for $\lambda = 0.5$ and $\lambda = 1.5$ respectively. For $\lambda = 0.5$, Figure 7 show that temperature rises as M increases. For $\lambda = 1.5$ in Figure 8, a decline in temperature profile is noticed for rise in M. Table **??** gives computed values proportional to the C_f and Nu for distinct entries of Chandershekhar number M and outer velocity parameter λ. Other than this, in Figure 8 (for $\lambda = 1.5$) the dispersion in the temperature profile curve for distinct magnitude of M is less as compared to Figure 7 (for $\lambda = 0.5$). The separation in temperature profile curves less because of the presence of greater outer velocity parameter λ. Hence, outer velocity parameter λ reduces the impact of M. Thus, to control the magnetic field in the flow, we use higher value of outer velocity parameter λ.

The influence of striking angle parameter γ on dimensionless velocity for $\lambda = 0.5$ and $\lambda = 1.5$ are displayed by images 9 and 10. Here, velocity profile increases with increasing the striking angle parameter

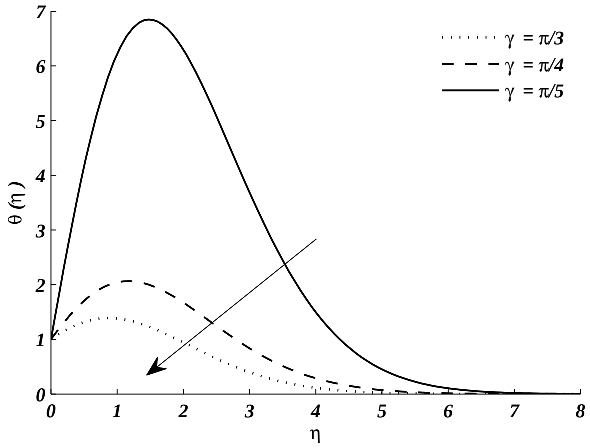

Figure 11: $\theta(\eta)$ for distinct γ, when $M = 0.1$, $R = 1$, $\beta = 0.5$, $Pr = 0.71$ and $\lambda = 0.5$.

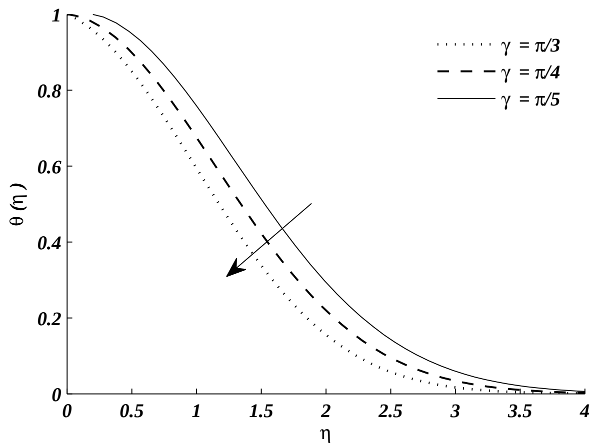

Figure 12: $\theta(\eta)$ for distinct γ, when $M = 0.1$, $R = 1$, $\beta = 0.5$, $Pr = 0.71$ and $\lambda = 1.5$.

γ. On the other hand, in Figure 10 for $\lambda > 1$, it has been observed that as we increase the striking angle parameter γ, the velocity profile is inverted.
Figures 11 and 12 show the influence of striking angle parameter γ on temperature profile for two situations of λ. In both situations, dimensionless temperature profile reduced for large value of striking angle parameter γ. Also, it has been noticed that in existence of greater outer velocity parameter λ (Figure 12), the effect of striking angle parameter γ is less with comparison of less outer velocity parameter λ (Figure 11). This effect of outer velocity parameter λ is observed by the separation of temperature profile curves in Figures 11 and 12.

4 Conclusions

The effectiveness of magnetic field and outer velocity over a stretching sheet on temperature and velocity profiles in Casson fluid have been studied. Numerical solutions are different fluid parameters has been shown in terms of temperature and velocity profiles. Major recommendations of the outcomes are compiled as below:

1. For $\lambda < 1$: (a) Velocity decreases with an increase in β and M, (b) Velocity increases with an increase in γ, (c) Temperature increases as we increase in β and M .(d) Reduced in temperature is noticed as γ increases.

2. For $\lambda > 1$: (a) Velocity rises with an rise in β, γ, and M (b) Temperature reduces for increase in β, γ and M, (c) An inverted boundary layer is formed in velocity profile.

References

[1] L. J. Crane, "Flow past a stretching plate," *Zeitschrift fr angewandte Mathematik und Physik ZAMP*, vol. 21, pp. 645–647, July 1970.

[2] H. I. Andersson, "MHD flow of a viscoelastic fluid past a stretching surface," *Acta Mechanica*, vol. 95, pp. 227–230, Mar. 1992.

[3] R. Cortell, "A note on magnetohydrodynamic flow of a power-law fluid over a stretching sheet," *Applied Mathematics and Computation*, vol. 168, pp. 557–566, Sept. 2005.

[4] V. Poply, P. Singh, and K. K. Chaudhary, "Analysis of laminar boundary layer flow along a stretching cylinder in the presence of thermal radiation," *WSEAS Trans Fluid Mech*, vol. 4, pp. 159–64, 2013.

[5] A. Ishak, K. Jafar, R. Nazar, and I. Pop, "MHD stagnation point flow towards a stretching sheet," *Physica A: Statistical Mechanics and its Applications*, vol. 388, pp. 3377–3383, Sept. 2009.

[6] P. Singh, N. S. Tomer, S. Kumar, and D. Sinha, "MHD oblique stagnation-point flow towards a stretching sheet with heat transfer," *International Journal of Applied Mathematics and Mechanics*, vol. 6, no. 13, pp. 94–111, 2010.

[7] P. Singh, A. Jangid, N. S. Tomer, and D. Sinha, "Effects of thermal radiation and magnetic field on unsteady stretching permeable sheet in presence of free stream velocity," *International Journal of Information and Mathematical Sciences*, vol. 6, no. 3, pp. 160–166, 2010.

[8] P. Singh, T. N. Singh, S. Kumar, and D. Sinha, "Effect of radiation and porosity parameter on magnetohydrodynamic flow due to stretching sheet in porous media," *Thermal Science*, vol. 15, no. 2, pp. 517–526, 2011.

[9] P. Singh, A. Kumar, N. S. Tomer, and D. Sinha, "Analysis of porosity effects on unsteady stretching permeable sheet," *Walailak Journal of Science and Technology (WJST)*, vol. 11, no. 7, pp. 611–620, 2013.

[10] V. Poply, P. Singh, and A. Yadav, "A Study of Temperature-dependent Fluid Properties on MHD Free Stream Flow and Heat Transfer over a Non-Linearly Stretching Sheet," *Procedia Engineering*, vol. 127, pp. 391–397, 2015.

[11] V. Poply, P. Singh, and A. K. Yadav, "Stability analysis of MHD outer velocity flow on a stretching cylinder," *Alexandria Engineering Journal*, June 2017.

[12] T. Hayat, M. Qasim, S. A. Shehzad, and A. Alsaedi, "Unsteady stagnation point flow of second grade fluid with variable free stream," *Alexandria Engineering Journal*, vol. 53, pp. 455–461, June 2014.

[13] P. G. Siddheshwar and N. Meenakshi, "Effects of Suction and Freestream Velocity on a Hydromagnetic Stagnation-Point Flow and Heat Transport in a Newtonian Fluid Toward a Stretching Sheet," *Journal of Heat Transfer*, vol. 138, no. 9, p. 094501, 2016.

[14] M. Subhas Abel, E. Sanjayanand, and M. M. Nandeppanavar, "Viscoelastic MHD flow and heat transfer over a stretching sheet with viscous and ohmic dissipations," *Communications in Nonlinear Science and Numerical Simulation*, vol. 13, pp. 1808–1821, Nov. 2008.

[15] I. Husain, F. Labropulu, and I. Pop, "Two-dimensional oblique stagnation-point flow towards a stretching surface in a viscoelastic fluid," *Open Physics*, vol. 9, Jan. 2011.

[16] M. S. Abel, P. Datti, and N. Mahesha, "Flow and heat transfer in a power-law fluid over a stretching sheet with variable thermal conductivity and non-uniform heat source," *International Journal of Heat and Mass Transfer*, vol. 52, pp. 2902–2913, May 2009.

[17] M. Mustafa, T. Hayat, P. Ioan, and A. Hendi, "Stagnation-Point Flow and Heat Transfer of a Casson Fluid towards a Stretching Sheet," *Zeitschrift fr Naturforschung A*, vol. 67, no. 1-2, pp. 70–76, 2014.

[18] P. K. Kameswaran, S. Shaw, and P. Sibanda, "Dual solutions of Casson fluid flow over a stretching or shrinking sheet," *Sadhana*, vol. 39, no. 6, pp. 1573–1583, 2014.

[19] K. Bhattacharyya, T. Hayat, and A. Alsaedi, "Exact solution for boundary layer flow of Casson fluid over a permeable stretching/shrinking sheet: Exact solution for flow of Casson fluid over a stretching/shrinking sheet," *ZAMM - Journal of Applied Mathematics and Mechanics / Zeitschrift fr Angewandte Mathematik und Mechanik*, vol. 94, pp. 522–528, June 2014.

[20] M. Sheikh and Z. Abbas, "Homogeneousheterogeneous reactions in stagnation point flow of Casson fluid due to a stretching/shrinking sheet with uniform suction and slip effects," *Ain Shams Engineering Journal*, vol. 8, pp. 467–474, Sept. 2017.

[21] A. M. Megahed, "Effect of slip velocity on Casson thin film flow and heat transfer due to unsteady stretching sheet in presence of variable heat flux and viscous dissipation," *Applied Mathematics and Mechanics*, vol. 36, pp. 1273–1284, Oct. 2015.

[22] Y. Lok, N. Amin, and I. Pop, "Non-orthogonal stagnation point flow towards a stretching sheet," *International Journal of Non-Linear Mechanics*, vol. 41, pp. 622–627, May 2006.